Table SI 1: Measurement conditions for the nanoparticle suspensions and corresponding ionic solutions.

Element	Line (nm)	c(metal) (µg L^{-1})	V (µL)	Device	Platform	Dosing
Gold	242	5	15	ContrAA600	Solid Sampling	manually
Silver	328	5	15	ContrAA600	Solid Sampling	manually
Platinum	265	50	20	ContrAA600	Integrated	MPE 60
Palladium	244	5	20	ContrAA600	Integrated	manually
Iron	248	20-50	20	ContrAA600	Integrated	manually
Gold E_a determination	242	5	20	NovAA800	Integrated	manually

Table SI 2: Furnace temperature program for Au nanoparticle analysis with ContrAA660

Step	Temperature (°C)	Heating rate (°C s^{-1})	Hold (s)
Drying I	80	6	20
Drying II	90	3	20
Drying III	110	5	20
Drying IIII	120	5	20
Pyrolysis I	350	50	20
Pyrolysis II	500	300	10
Auto-zero	500	0	5
Atomization	2200	1500	5
Cleaning	2450	500	4

Table SI 3. Furnace temperature program for Au nanoparticle analysis with NovAA 800.

Step	Temperature (°C)	Heating rate (°C s^{-1})	Hold (s)
Drying I	80	6	20
Drying II	90	3	20
Drying III	110	5	20
Drying IV	120	5	10
Pyrolysis I	150	50	10
Pyrolysis II	850	700	1
Auto-zero	850	0	6
Atomization	2200	250	0
Cleaning	2450	500	4

Table SI 4: Furnace temperature program for Ag analysis.

Step	Temperature (°C)	Heating rate (°C s^{-1})	Hold (s)
Drying I	80	6	20
Drying II	90	3	20
Drying III	110	5	20
Drying IIII	120	5	20
Pyrolysis I	350	50	20
Pyrolysis II	400	300	10

Step	Temperature (°C)	Heating rate (°C s⁻¹)	Hold (s)
Auto-zero	400	0	5
Atomization	1800	1500	3
Cleaning	2450	500	4

Table SI 5: Furnace temperature program for Pt analysis.

Step	Temperature (°C)	Heating rate (°C s⁻¹)	Hold (s)
Drying I	80	6	20
Drying II	90	3	20
Drying III	110	5	10
Pyrolysis I	350	50	20
Pyrolysis II	1300	300	10
Auto-zero	1300	0	5
Atomization	2400/2400/2200	1500/500/1500	6
Cleaning	2500	500	4

Table SI 6: Furnace temperature program for Pd analysis.

Step	Temperature (°C)	Heating rate (°C s⁻¹)	Hold (s)
Drying I	80	6	20
Drying II	90	3	20
Drying III	110	5	10
Pyrolysis I	350	50	20
Pyrolysis II	950	300	10
Auto-zero	950	0	5
Atomization	2400/2400/2200	1500/250/1500	6
Cleaning	2450	500	4

Table SI 7: Furnace temperature program for Fe analysis.

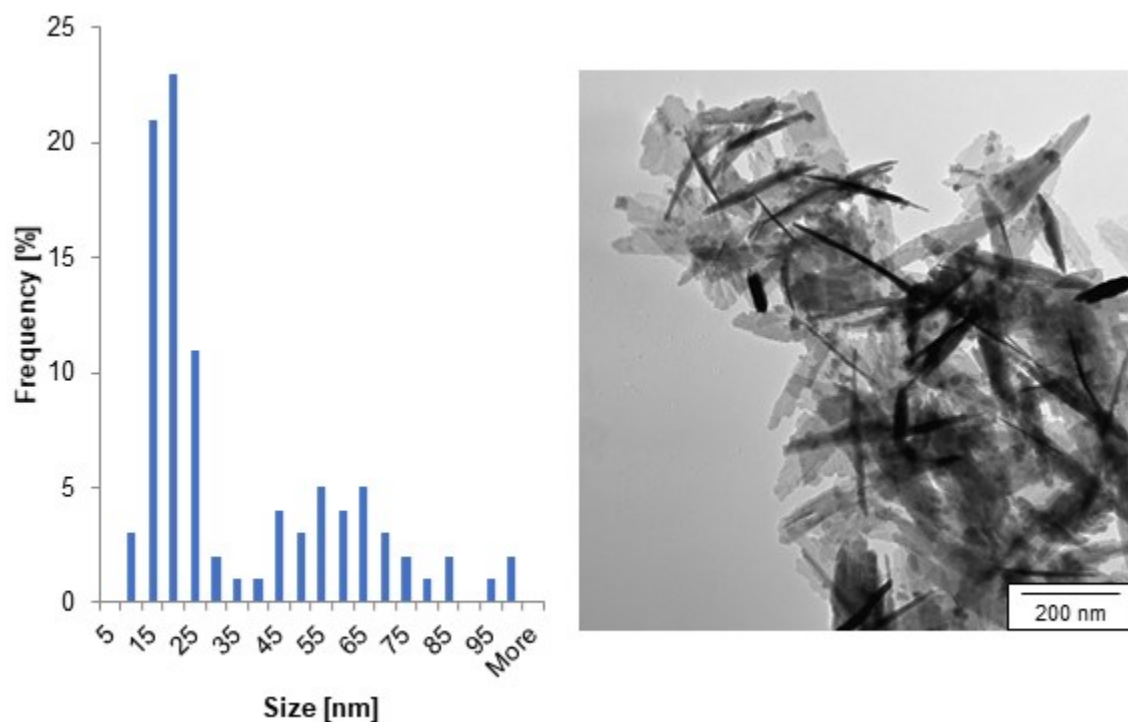| Step	Temperature (°C)	Heating rate (°C s⁻¹)	Hold (s)
Drying I	80	6	20
Drying II	90	3	20
Drying III	110	5	10
Pyrolysis I	350	50	20
Pyrolysis II	950	300	10
Auto-zero	950	0	5
Atomization	2100	1500	8
Cleaning	2450	500	4

Figure SI 1: Size distribution of nZVI and exemplary TEM image (n = 94).

Table SI 8: Potential depth parameter of Lennard-Jones potential for interaction between metal and carbon. Displayed parameters were calculated with Lorenzt-Berthold (LB) rule[1–3] and found in literature.

Compound	Potential depth ε (eV)	
	Calculated by LB rule	Found in literature
Ag-C	0.0291	0.0301[4,5]
Au-C	0.0332	0.01273-0.0341[5–8]
Pd-C	0.0335	0.0335-0.03444[8,9]
Fe-C	0.0357	0.02495[10,11]
Pt-C	0.0409	0.04092[8,12]
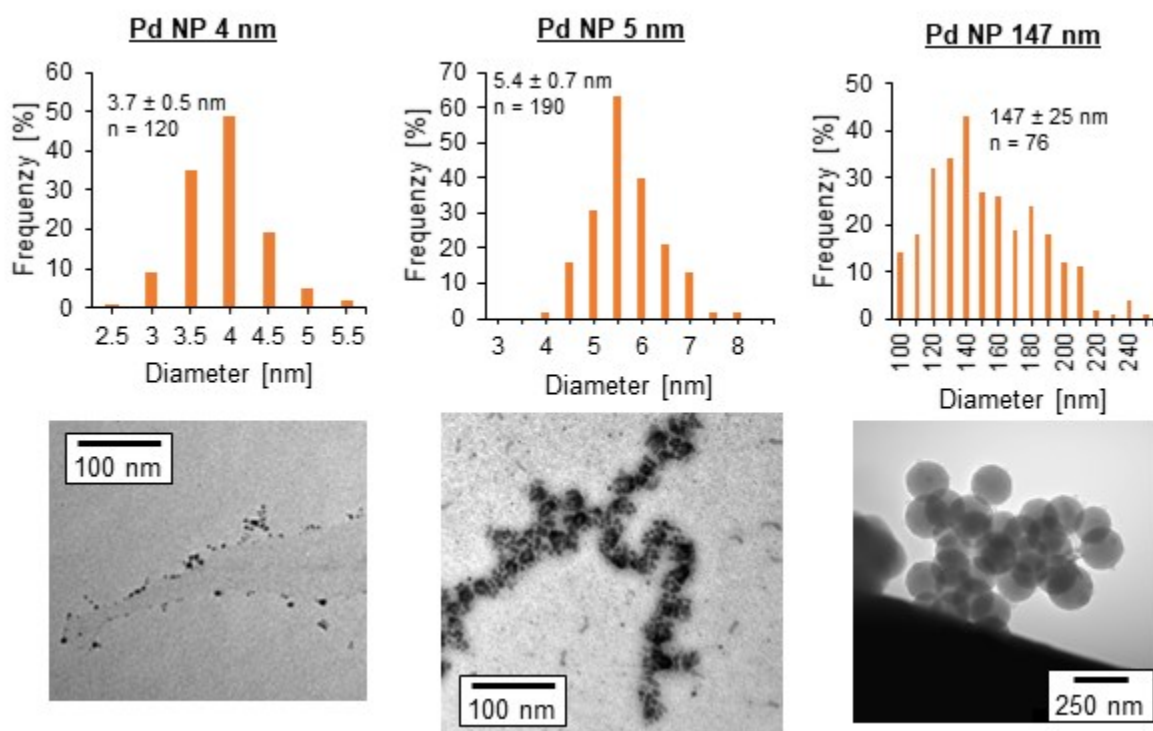
Figure SI 2. Exemplary TEM images and size distributions of synthesized Pd NPs.
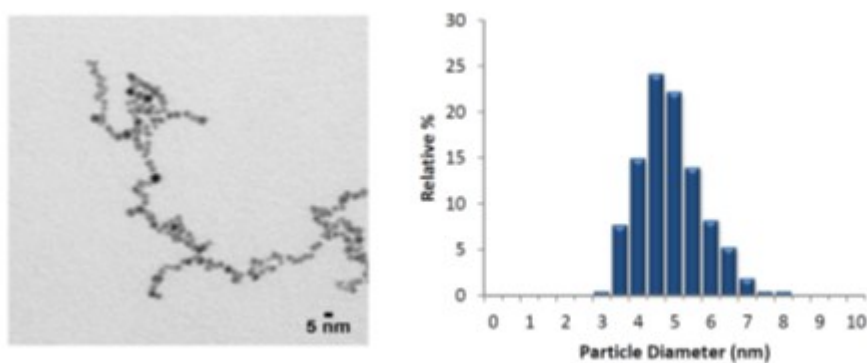
Figure SI 3: Exemplary TEM image and size distribution of Pt NP sized 5 nm. Data were provided as certificate of analysis by the manufacturer.
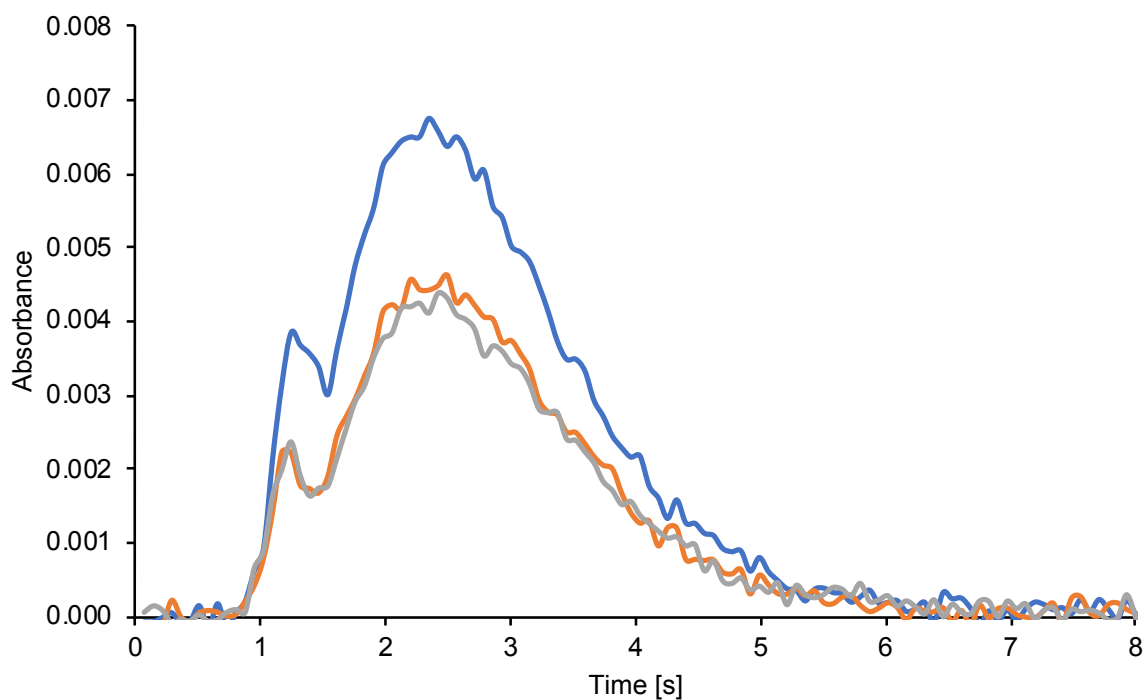
Figure SI 4: Absorbance signal of ionic Pd (blue), Pd NP 4 nm (orange) and Pd NP 150 nm (grey) atomized in the presence of ruthenium modifier.
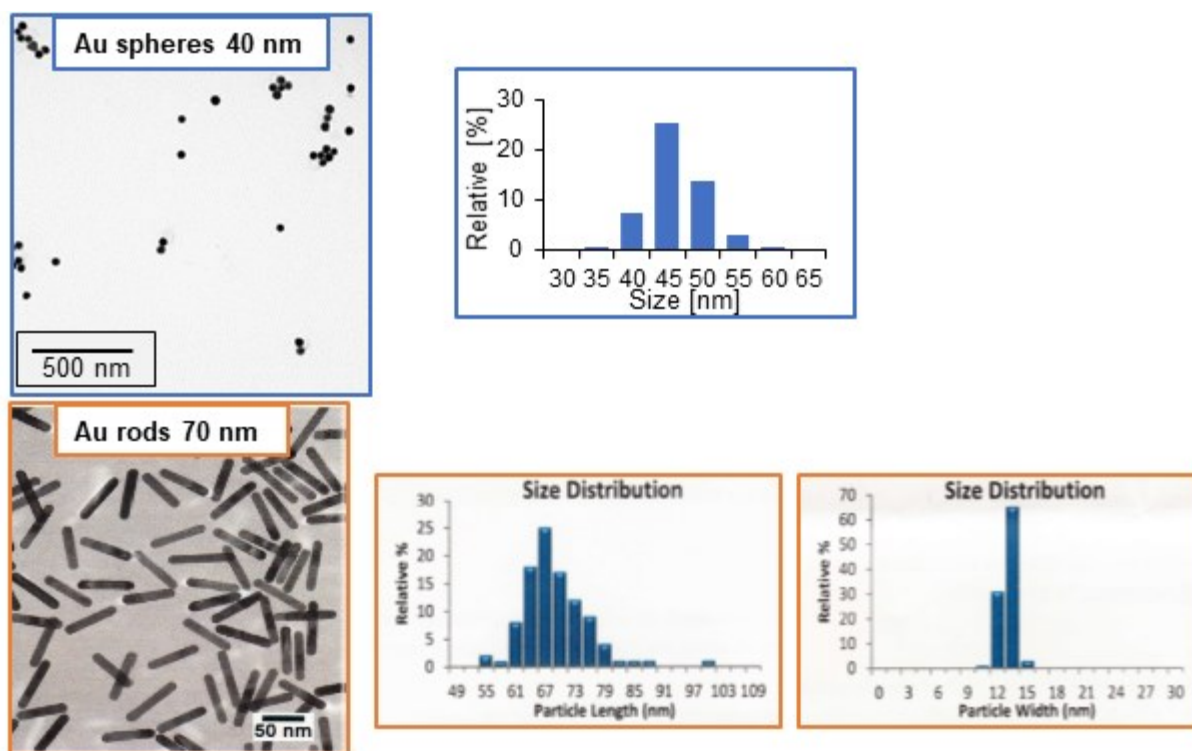

Figure SI 5: Exemplary TEM images and size distribution of Au spheres and Au rods. Data for Au rods were provided as certificate of analysis by the manufacturer, while data for Au spheres were measured by TEM.
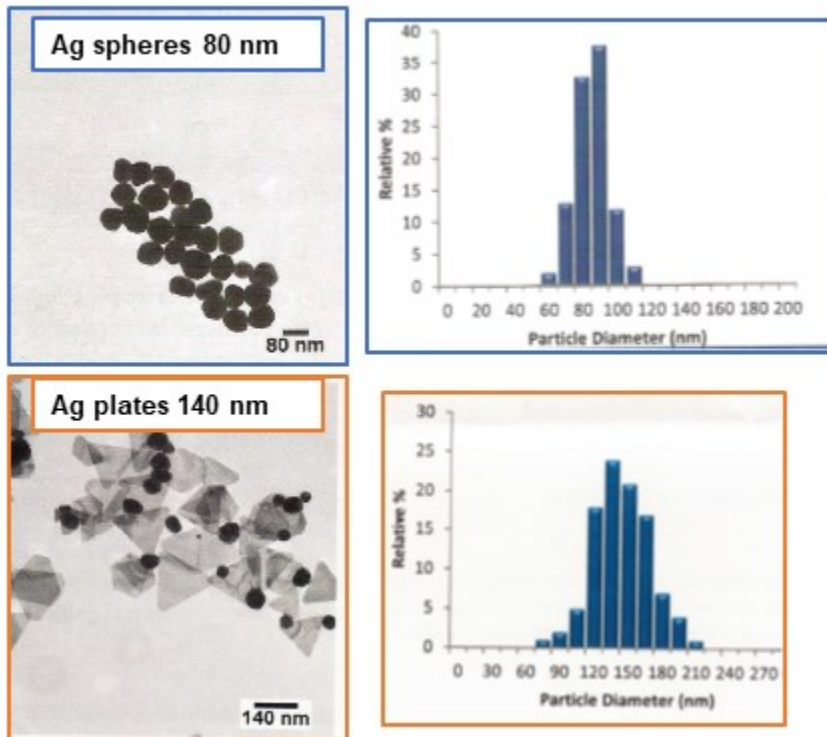
Figure SI 6: Exemplary TEM images and size distribution of Ag spheres and Ag plates. Data were provided as certificate of analysis by the manufacturer.
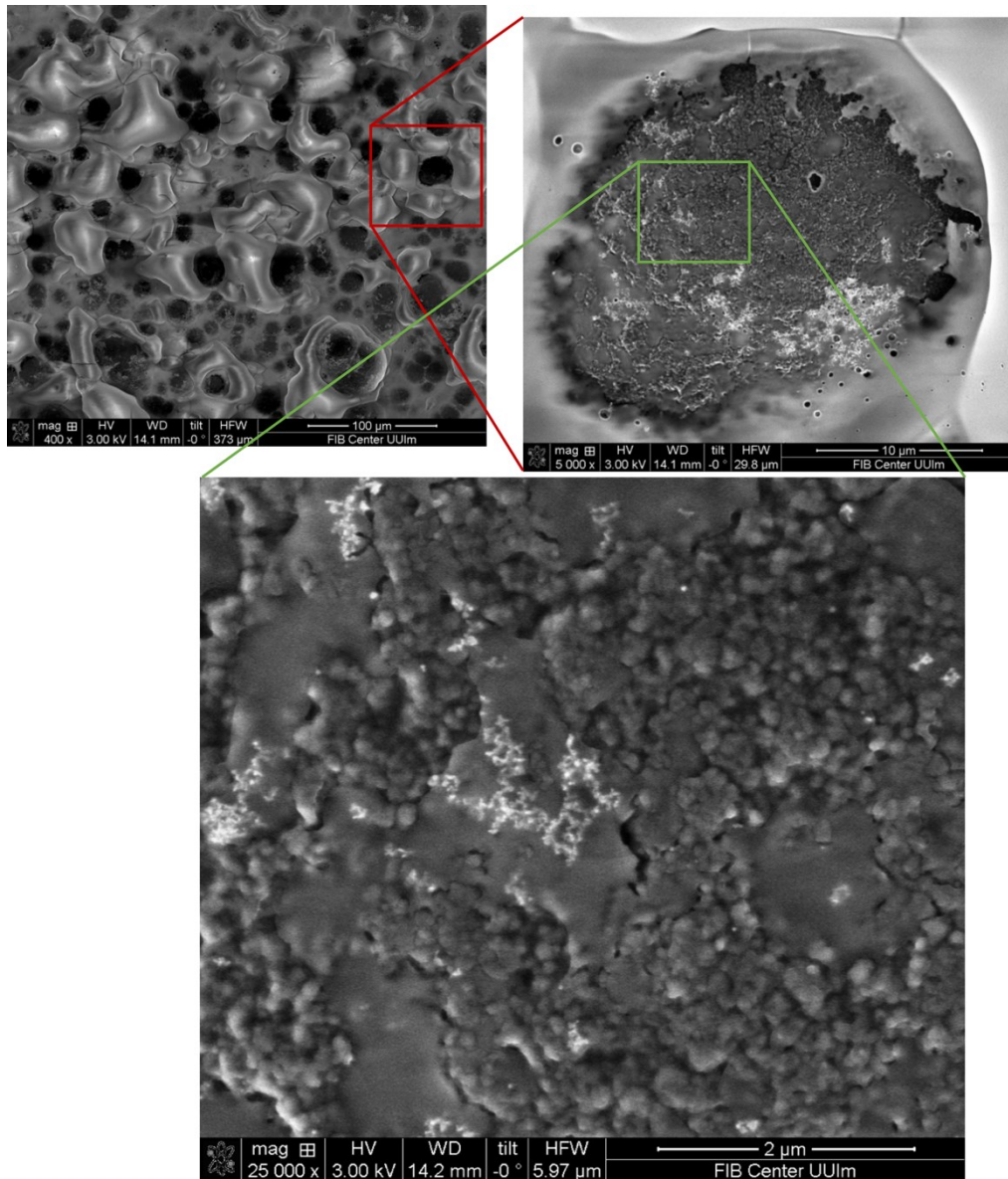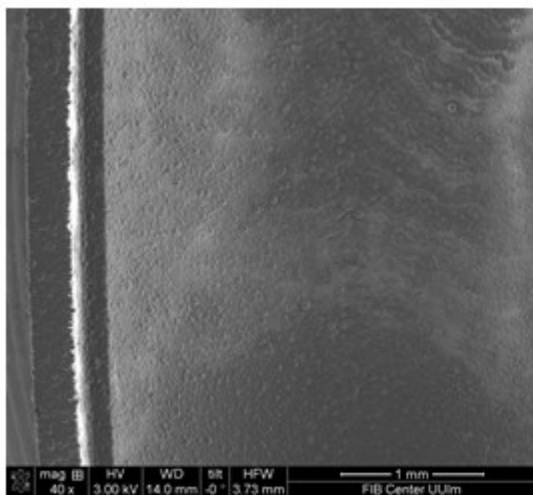
Figure SI 7: Exemplary SEM images of Ag Plates 32 nm on solid sampler graphite platform.
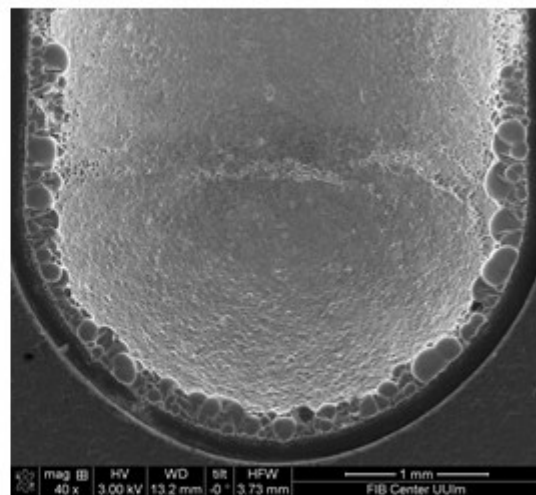
Figure SI 8: Exemplary SEM images of graphite platform with a) Au rods stored in UPW and b) Ag plates stored in aqueous 5 mM sodium borate. In Figure b) the crystallized sodium borate is visible.

Literature:

1 P. M. Agrawal, B. M. Rice and D. L. Thompson, *Surface Science*, 2002, **515**, 21–35.

2 L. Miao, V. R. Bhethanabotla and B. Joseph, *AIChE Annual Meeting, Conference Proceeding*, 2004, 2453–2460.

3 L. Xie, P. Brault, A.-L. Thomann and J.-M. Bauchire, *Applied Surface Science*, 2013, **285**, 810–816.

4 H. Akbarzadeh and H. Yaghoubi, *Journal of Colloid and Interface Science*, 2014, **418**, 178–184.

5 M. Neek-Amal, R. Asgari and M. R. R. Tabar, *Nanotechnology*, 2009, **20**, 135602.

6 C. H. Claassens, J. J. Terblans, M. J. H. Hoffman and H. C. Swart, *Surface and Interface Analysis*, 2005, **37**, 1021–1026.

7 W. D. Luedtke and U. Landman, *Phys. Rev. Lett.*, 1999, **82**, 3835–3838.

8 H. Wei, S. Wei, X. Zhu and X. Lu, *J. Phys. Chem. C*, 2017, **121**, 12911–12920.

9 D. Schebarchov, S. C. Hendy and W. Polak, *J. Phys.: Condens. Matter*, 2009, **21**, 144204.

10 Y. Yin, W. Li, H. Shen, J. Zhou, H. Nan, M. Deng, X. Shen and Z. Tu, *ISIJ International*, 2018, **58**, 1022–1027.

11 J. P. Ewen, C. Gattinoni, F. M. Thakkar, N. Morgan, H. A. Spikes and D. Dini, *Tribol Lett*, 2016, **63**, 38.

12 D. Cheng, W. Wang and S. Huang, *J. Phys. Chem. C*, 2007, **111**, 1631–1637.